Analyzing Hydrogen Recombination Lines in the Infrared and Optical to Determine Extinction and SFRs of Dusty Infrared Galaxies

Anna V. Payne,[1,2] Hanae Inami,[1] Matthew A. Malkan,[3] Hideo Matsuhara,[4] and Shoko Sakai[3]

[1] *Univ Lyon, Univ Lyon1, Ens de Lyon, CNRS, Centre de Recherche Astrophysique de Lyon (CRAL) UMR5574, F-69230, Saint-Genis-Laval, France*

[2] *Institute for Astronomy, University of Hawai'i at Manoa, 2680 Woodlawn Dr, Honolulu, HI 96822, USA*

[3] *Department of Physics & Astronomy, University of California Los Angeles, Los Angeles, CA 90095, USA*

[4] *Institute of Space and Astronautical Science, JAXA, Sagamihara, Kanagawa 252-5210, Japan*

ABSTRACT

Star formation rate (SFR) is important to quantify for galaxies because it provides a method for reconstructing the cosmic history of star formation in the universe. $H\alpha$ is frequently utilized in SFR studies, however, this hydrogen recombination line is strongly affected by interstellar dust extinction. For a sample of 23 galaxies, we report $\frac{Br\alpha}{H\alpha}$ and $\frac{H\alpha}{H\beta}$ measurements and found that for most of our sample, the traditional Balmer decrement, $\frac{H\alpha}{H\beta}$, unexpectedly gives higher A_V than when $\frac{Br\alpha}{H\alpha}$ is used when we adopt the Calzetti extinction law. In addition, galaxies with the highest specific star formation rate (SSFR) on average have higher $A_V(\frac{Br\alpha}{H\alpha})$ than $A_V(\frac{H\alpha}{H\beta})$. However, we do not find a clear trend of the line ratios against L_{IR} or $\frac{IR}{UV}$.

Keywords: interstellar dust extinction, star formation rate, luminous infrared galaxy

1. INTRODUCTION

$H\alpha$ can be considered the "gold standard" in SFR research because this line is a direct probe of ionizing photons and is easily observed from ground-based facilities, up to $z = 2.72$. For this reason, $H\alpha$ is frequently utilized. However, $H\alpha$ is strongly affected by interstellar dust extinction, therefore, using $H\alpha$ possibly introduces a source of error in finding SFRs. Determining more accurate SFRs require a precise reddening correction factor. Currently, the Balmer decrement, $\frac{H\alpha}{H\beta}$, is widely used to estimate interstellar dust extinction.

Our goal was to observe hydrogen recombination lines at longer wavelengths where extinction is reduced compared to $H\alpha$. Brackett-α, at 4.05 μm, is one such hydrogen line. Perhaps $Br\alpha$ can be considered the "platinum standard." *AKARI* has enabled us to access $Br\alpha$ at 4.05 μm which cannot be transmitted through the atmosphere. If a large percentage of $H\alpha$ and $H\beta$ is being absorbed by dust through this high degree of extinction, then we only have information about the outer part of a dusty cloud. $Br\alpha$ has the potential to penetrate from deeper dust clouds compared to $H\alpha$. We have investigated the potential for $\frac{Br\alpha}{H\alpha}$ to be utilized as a more precise indicator for extinction.

2. SAMPLE AND DATA

Infrared observations were taken using *AKARI* with Np aperture pointing observations during the post-helium (warm phase) mission. Optical observations were taken at the Lick Observatory using the Kast Double Spectrograph between 2009–2014. Our sample of 23 galaxies covers a wide range of L_{IR} from $\log\left(\frac{L_{\mathrm{IR}}}{L_\odot}\right) = 10$ to 12. Half of the galaxies in the sample are from the GOALS project (Great Observatories All-sky LIRG Survey, Armus et al. 2009) which studied low-redshift luminous infrared galaxies (LIRGs) by combining space-borne observatory data into a comprehensive imaging and spectroscopic survey. All target galaxies from this research are shown in Table 1 and are located in the local universe ($z < 0.1$).

3. DATA PROCESSING AND ANALYSIS

The extraction sizes of the *AKARI* and Lick spectra were matched to ensure a one-to-one comparison for each galaxy's total emission. Example spectra for IRAS03359+1523 are shown in Figure 1 with an SDSS image indicating the slit positions and slit size of the Kast Double spectrograph. *AKARI*'s dispersion direction is denoted with a red arrow. L_{IR},

Corresponding author: Anna V. Payne
avpayne@hawaii.edu

Table 1. The target galaxies analyzed.

GOALS sources	Merger State/AGN	$\log\left(\frac{L_{IR}}{L_\odot}\right)$
(a) IRAS17132+5313	Early stage merger	11.94
(b) IRAS09111-1007W	Early stage merger	11.90
(c) NGC2623	Late-stage merger, AGN	11.58
(d) IC5298	Non-merger, AGN	11.57
(e) IRAS03359+1523	Late-stage merger	11.56
(f) NGC6090	Mid-stage merger	11.53
(g) NGC5256	Early-stage merger, AGN	11.52
(h) Arp256	Early-stage merger	11.45
(i) NGC4922	Mid-stage merger, AGN	11.35
(j) CGCG453-062	Non-merger	11.34
(k) UGC12150	Non-merger	11.30
(l) IRAS09111-1007E	Early stage merger	11.24
Non-GOALS sources	**Galaxy Type**	$\log\left(\frac{L_{IR}}{L_\odot}\right)$
(m) GIN86	Seyfert 2	11.62
(n) MCG+08-30-009	Emission-line galaxy	11.61
(o) Leda90208	Radio galaxy	11.28
(p) IRAS00353-0641	Unclassified galaxy	11.24
(q) UGC11865	Compact elliptical	11.23
(r) IC1228	Spiral barred	11.10
(s) Mrk839	Starburst	10.73
(t) UGC9922	Pair of galaxies	10.70
(u) CGCG415-038	Lenticular	10.53
(v) MCG+08-13-076	Non-merger galaxy in cluster	10.17
(w) KUG0153+370	Spiral barred	10.08

Note— Column 1: source name from NED; Column 2: Merger stages obtained from Stierwalt et al. (2013) for the GOALS sources, and galaxy type obtained from NED for non-GOALS sources; Column 3: Total $\log\left(\frac{L_{IR}}{L_\odot}\right)$ computed using the *IRAS* flux densities reported in the RBGS for GOALS galaxies and FSC for non-GOALS galaxies and luminosity distance computed using a cosmology of $\Omega_\Lambda = 0.72$, $\Omega_m = 0.28$, with $H_0 = 70$ km s^{-1} Mpc^{-1}, $\log\left(\frac{L_{IR}}{L_\odot}\right)$ for (b) and (l) obtained from Howell et al. (2010).

$\frac{IR}{UV}$, and SSFR were determined for each galaxy based on the ancillary IRAS, Spitzer, and and GALEX data, following Armus et al. (2009) and Howell et al. (2010).
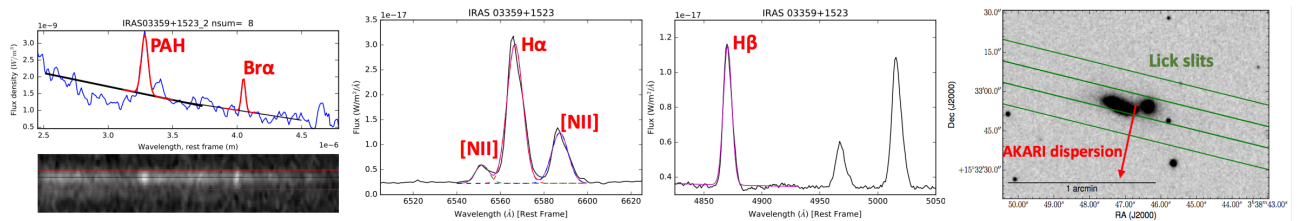

Figure 1. *AKARI* spectra for galaxy IRAS03359+1523 showing the fit for PAH at 3.33 μm and Brα at 4.05 μm, followed by spectra taken at Lick Observatory showing the fit for Hα and the [N II] doublet, and Hβ, followed by an SDSS image showing the slit positions and slit size for the Kast Double spectrograph. *AKARI*'s dispersion direction is denoted with a red arrow.

4. RESULTS

Comparing $\frac{Br\alpha}{H\alpha}$ and $\frac{H\alpha}{H\beta}$ ratios directly provides differences in the dust extinction measured at longer and shorter wavelengths. We found that for most of our sample, the traditional Balmer decrement, $\frac{H\alpha}{H\beta}$, gives higher A_V than when $\frac{Br\alpha}{H\alpha}$ is used (Figure 2), assuming the Calzetti extinction curve (Calzetti et al. 2000). A steeper extinction curve in the visible range can reduce the inconsistency of A_V measured in these flux ratios. For a steeper curve in the visible range, at a given $H\alpha$, a higher $H\beta$ is expected, but not much for $H\alpha$ at a given $Br\alpha$. This can reduce the estimated $A_V(\frac{H\alpha}{H\beta})$, while keeping $A_V(\frac{Br\alpha}{H\alpha})$ the same.

Interestingly, we also find that the galaxies with the highest SSFRs (Figure 3, right), which have more intense star formation, and potentially more dusty environments, on average have higher $\frac{Br\alpha}{H\alpha}$ than $\frac{H\alpha}{H\beta}$. Thus, for galaxies with high SSFRs, it may be more likely to underestimate their dust extinction when $\frac{H\alpha}{H\beta}$ is used. However, we do not find a clear trend of the line ratios against L_{IR} (Figure 3, left) or $\frac{IR}{UV}$ (Figure 3, center).
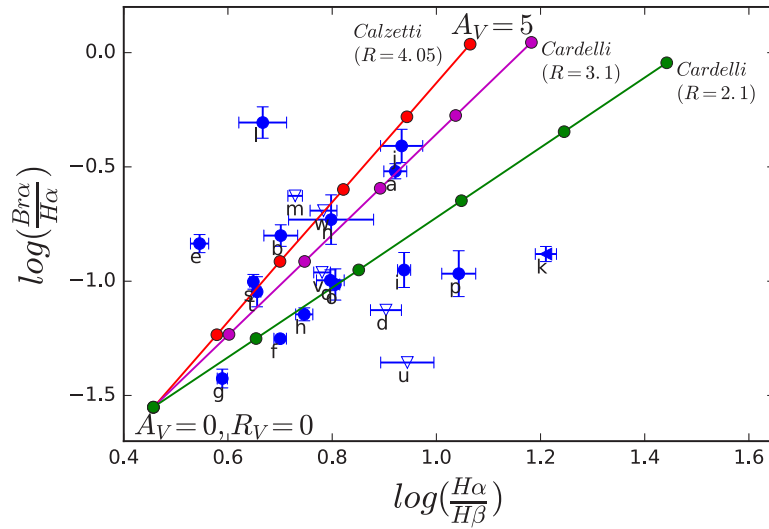
Figure 2. $\log\left(\frac{Br\alpha}{H\alpha}\right)$ vs. $\log\left(\frac{H\alpha}{H\beta}\right)$ for the galaxies shown in Table 1. The red A_V line assumes the Calzetti extinction curve ($R = 4.05$, Calzetti et al. 2000). The Calzetti curve was extrapolated to $4.05\,\mu$m for $Br\alpha$ and for the intrinsic line ratios Case B is assumed, $T = 10,000$ K, $n_e = 100$ cm^{-3}. The A_V line has a step of 1 magnitude. Purple and green lines indicate the Milky Way attenuation curve with $R_V = 3.1$ and $R_V = 2.1$ (Cardelli et al. 1989). The open symbols are upper limits.

left	center	right
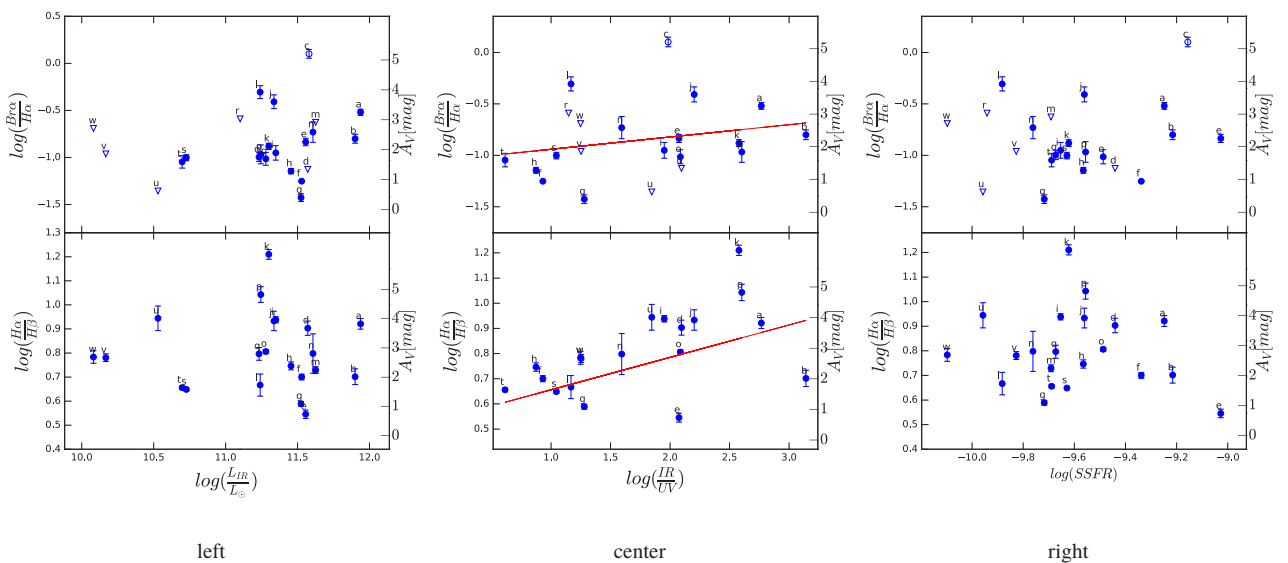
Figure 3. $\log\left(\frac{Br\alpha}{H\alpha}\right)$ and $\log\left(\frac{H\alpha}{H\beta}\right)$ vs. $\log\left(\frac{L_{IR}}{L_\odot}\right)$, $\log\left(\frac{IR}{UV}\right)$, and $\log(\text{SSFR})$ calculated for each galaxy shown in Table 1.

5. SUMMARY

We report on measurements for dust extinction for a sample of 23 galaxies. Infrared observations taken using *AKARI* were used to obtain measurements for Brα, and optical observations taken using the Kast Double Spectrograph at Lick Observatory were used to obtain measurements for Hα and Hβ. Comparing $\frac{Br\alpha}{H\alpha}$ and $\frac{H\alpha}{H\beta}$, we found that for most of our sample, the traditional Balmer decrement, $\frac{H\alpha}{H\beta}$, unexpectedly gives higher A_V than when $\frac{Br\alpha}{H\alpha}$ is used when we adopt the Calzetti extinction law. A steeper extinction curve in the visible range can reduce the inconsistency of A_V measured in these flux ratios. We do not find a clear trend of the line ratios against L_{IR} or $\frac{IR}{UV}$, but we find that the galaxies with the highest SSFRs, with more intense star formation, on average have higher $\frac{Br\alpha}{H\alpha}$ than $\frac{H\alpha}{H\beta}$. Thus, for galaxies with high SSFRs, it may be more likely to underestimate their dust extinction when $\frac{H\alpha}{H\beta}$ is used.

ACKNOWLEDGMENTS

REFERENCES

Armus, L., Mazzarella, J. M., Evans, A. S., et al. 2009, PASP, 121, 559
Calzetti, D., Armus, L., Bohlin, R. C., et al. 2000, ApJ, 533, 682
Cardelli, J.A., Clayton, G.C., Mathis, J.S. 1989, ApJ, 345, 245
Howell, J. H., Armus, L., Mazzarella, J. M., et al. 2010, ApJ, 715, 572
Stierwalt, S., Armus, L., Surace, J. A., et al. 2013, ApJS, 206, 1